Journal of Materials Chemistry C

ROYAL SOCIETY OF CHEMISTRY

PAPER

View Article Online
View Journal



Cite this: DOI: 10.1039/d2tc05139g

# A cross-linkable, organic down-converting material for white light emission from hybrid LEDs†

Hao Yang,[a] Jochen Bruckbauer,[b] Lyudmyla Kanibolotska,[a] Alexander L. Kanibolotsky,[ac] Joseph Cameron,[a] David J. Wallis,[de] Robert W. Martin*[b] and Peter J. Skabara*[a]

Received 2nd December 2022,
Accepted 24th April 2023

DOI: 10.1039/d2tc05139g

rsc.li/materials-c

The use of organic materials and the replacement of rare-earth elements in the making of light-emitting devices has been increasingly popular over the last decades. Herein, the synthesis and characterisation of a novel organic green-emitting material (**GreenCin**), based on a fluorene-benzothiadiazole-fluorene (Flu-BT-Flu) core structure, and its performance as a down-converting layer in tandem with commercial blue light-emitting diodes (LEDs) for white light emission are reported. This material has been functionalised with cinnamate-groups to enable the emissive material to react with the cross-linker tetra(cinnamoyloxymethyl)methane (**TCM**), to produce stable films with high performance in hybrid LEDs. The hybrid devices can generate white light with a good colour rendering index (CRI) of 69. The hybrid devices also have ×2.6 increased luminous efficacy (107 lm $W^{-1}$) and ×2.4 increased radiant flux (24 mW) when compared with hybrid devices using non-cross-linked analogues of **GreenCin**. Additionally, the hybrid devices containing **GreenCin** have a high blue-to-white efficacy value (defined by dividing the luminous flux of a hybrid device by the radiant flux of the underlying blue LED), of 213 lm $W^{-1}$, for which inorganic phosphors have values in the range of 200–300 lm $W^{-1}$.



## 1. Introduction

With the booming industrial needs for high performance displays and lighting devices, it is crucial to achieve higher white light output efficiencies.[1] Commonly, white light-emitting diodes (WLEDs) can be produced through a combination of inorganic LEDs that emit at different colour ranges or by coating inorganic LEDs that emit at blue, violet, or near-UV range with down-converting inorganic phosphors.[2,3] White light-emitting devices that consist of a combination of inorganic red, green, and blue (RGB) LEDs offer higher values for the colour rendering index (CRI) but come with high manufacturing and maintenance costs.[2] These inorganic LEDs can produce white light with CRI values of over 80.[4,5] However, their performance is commonly hindered by the need to balance the output from three separate LEDs and the lack of efficient green output. This is a problem due to how well human eyes respond to green light.[6,7]

To solve these problems, inorganic phosphors can be used as down-converting materials to coat inorganic LEDs and to achieve white light emission.[8–15] Commercially, the most popular approach is to combine blue LEDs with inorganic phosphors that absorb a portion of the blue light and emit in the yellow region so that the combination of transmitted blue and emitted yellow appears as white light.[16,17] The colour rendering can also be further improved by adding red phosphors to increase the emission coverage. However, despite good device performance through the use of inorganic phosphors, several drawbacks still exist. The synthesis of inorganic phosphors usually involves the use of rare-earth elements such as yttrium (Y), cerium (Ce), gadolinium (Gd), and ytterbium (Yb), which increases the manufacturing costs.[18,19] In addition, WLEDs with inorganic phosphors tend to have low colour rendering capability due to the weak green and red emission.[20] Finally, the device performance is further hindered due to self-absorption which causes photoluminescence quenching in inorganic phosphors.[21]

By comparison, organic materials used as the emissive layers in organic light-emitting diodes (OLEDs) possess distinct

[a] WestCHEM, School of Chemistry, University of Glasgow, Glasgow, G12 8QQ, UK. E-mail: peter.skabara@glasgow.ac.uk
[b] Department of Physics, SUPA, University of Strathclyde, Glasgow, G4 0NG, UK. E-mail: r.w.martin@strath.ac.uk
[c] Institute of Physical-Organic Chemistry and Coal Chemistry, 02160 Kyiv, Ukraine
[d] Department of Materials and Metallurgy, University of Cambridge, Cambridge, CB3 0FS, UK
[e] Centre for High Frequency Engineering, University of Cardiff, Cardiff, CF24 3AA, UK

† Electronic supplementary information (ESI) available. See DOI: https://doi.org/10.1039/d2tc05139g

characteristics such as low manufacturing costs, ease of synthesis and colour tuning of emission, together with mechanical flexibility.[22–24] However, they also exhibit some distinct problems which hinder the complete substitution of inorganic components. Organic materials tend to aggregate when in the solid state, which can quench the emission. Additionally, organic materials suffer from inferior stability under device operation conditions that can cause OLEDs to have relatively short device lifetimes when compared to their inorganic counterparts.[24]

To solve this issue, the design of hybrid inorganic/organic LED devices has been proposed to potentially combine the advantages of both inorganic LEDs and organic materials. Most commonly, this hybrid architecture is achieved by having an organic material coating as a frequency down-converter for an inorganic LED.[25–29] One of the early works on white light-emitting devices that combines an inorganic LED with an organic material was conducted by Hide *et al.*[30] In this work, InGaN LEDs that emit in the blue region were coated with two organic polymers as a bilayer that emit within the green (BuEH-PPV) and red (MEH-PPV) regions of the visible spectrum. In general, the colour of the overall emission can be tuned by varying the thickness of each organic layer to achieve an 'ideal' value. The commission internationale de l'éclairage (CIE) coordinates of the 'whitest' device is (0.34, 0.29), which is close to the most ideal white point of equal-energy that is located at (0.33, 0.33).

Previously, we reported a hybrid inorganic/organic LED device that utilises a yellow-emitting material as an energy down-converter for a blue LED.[26] The organic down-converter material was dissolved and cured in a 1,4-cyclohexanedimethanol divinyl ether (CHDV) matrix to give a rigid membrane that forms a dome on the blue LED and serves to provide some stability from air for the organic emitter. Embedding organic down-converters in additional solid matrices can disaggregate the organic dyes and limit the π–π stacking.[31,32] However, in order to form a CHDV matrix, a photoacid generator, 4-octyloxy diphenyliodonium hexafluoroantimonate (PAG), is needed to initiate the cross-linking process. PAG is sensitive to short UV wavelength (250 nm) and decomposes during illumination to release protons. The vinyl ether units polymerise due to the presence of protons which eventually leads to the cross-linked matrix network. Although the CHDV matrix can embed the organic material well to prevent photo-oxidation, the degree of cross-linking is rather difficult to control. In addition, we observed that the colour of the membranes has the tendency to change to deep yellow over time with higher PAG concentration, which consequently lowers the down-converting efficiency. CHDV encapsulation was also used for organic light emitting materials based on 2,1,3-benzothiadiazole-fluorene (BT-Flu) core structures. Taylor-Shaw *et al.* reported novel organic down-converting materials, $(TPA\text{-}Flu)_2BT$ and $(TPA\text{-}Flu)_2$-BTBT, that emit in the yellow region and were integrated with a blue LED.[33] The materials served well as down-converting materials for blue LEDs with a highest luminous efficacy value of 41 lm $W^{-1}$ and CIE coordinates of (0.34, 0.31).

Herein, we report a novel organic green-emitting material (**GreenCin**) which has the advantage that it can be used as an energy down-converter for blue LEDs with high efficiency and also can be applied to blue LEDs as a homogeneous layer without the need of additives in the host matrix materials for encapsulation due to the photoreactive properties of cinnamate groups (Fig. 1). Apart from the photoreactive ability, this material also bears several distinct characteristics—it has an absorbance band that aligns closely with the emission wavelength of blue LEDs and it has a high photoluminescence quantum yield (PLQY) that can lead to higher luminous efficacy values. The material is based on a well-studied green-emitter structure that consists of an electron-deficient BT core flanked by two fluorene units as weak electron donors. The BT-Flu backbone structure is known for its effectiveness as a green-emitter.[34] The UV-curability comes from the cinnamate functionality at the end of each fluorene unit. Cinnamate groups are known to undergo a [2+2] cycloaddition reaction under UV irradiation to form a cyclobutane ring structure due to the vinyl groups.[35] However, due to the linear structure of **GreenCin**, the polymeric form is also linear. In order to cross-link **GreenCin** to form a robust matrix, tetra(cinnamoyloxymethyl)methane (**TCM**) was added as a cross-linking agent (Fig. 1). The resulting cross-linked **GreenCin** film is insoluble in most organic solvents, which makes it a physically stable film without the need of additional encapsulation, as well as being a promising candidate as an energy down-converting coating for use with blue LEDs. The resulting devices demonstrate very reasonable colour rendering quality ($52 < CRI < 69$) and a high luminous efficacy value of 107 lm $W^{-1}$, as well as an excellent blue-to-white efficacy value of 213 lm $W^{-1}$ (defined by dividing the luminous flux of a hybrid device by the radiant flux of the underlying blue LED). The blue-to-white efficacy value can be used to determine the amount of white light output from the

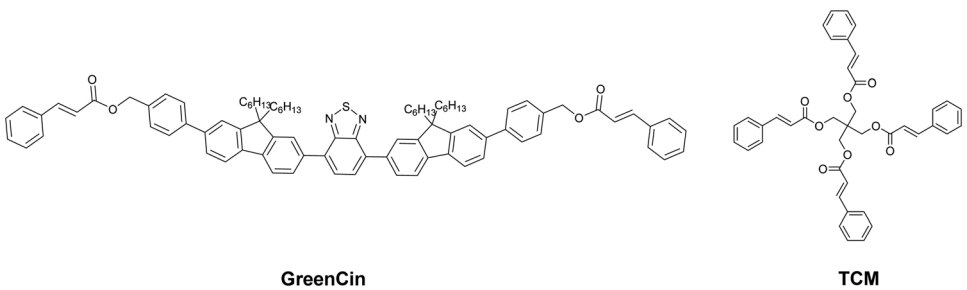


Fig. 1 The structures of GreenCin and TCM.

 

devices that is generated by colour conversion of the absorber/emitter. By comparison, the blue-to-white efficacy values of commonly used commercial phosphors range between 200–300 lm $W^{-1}$.[3]

## 2. Synthesis

The syntheses of **TCM**,[36] tetrakis(triphenylphosphine)palladium,[37] 9,9-dihexyl-7-trimethylsilylfluoren-2-yl boronic acid (**2**), 4,7-bis(7-trimethylsilyl-9,9-dihexylfluoren-2-yl)-2,1,3-benzothiadiazole (**3**) and 4,7-bis(7-bromo-9,9-dihexylfluoren-2-yl)-2,1,3-benzothiadiazole (**4**)[33] are described in the literature. **GreenCin** was synthesised in 5 steps according to the following procedure (Scheme 1). 2,7-Dibromo-9,9-dihexylfluorene (**1**) was functionalised with a trimethylsilane group and a boronic acid group at the brominated positions in two sequential steps to give 9,9-dihexyl-7-trimethylsilylfluoren-2-yl boronic acid **2**. The dibromo-BT unit was then coupled with the modified fluorene unit **2** *via* a Suzuki-coupling reaction to yield 4,7-bis(7-trimethylsilyl-9,9-dihexylfluoren-2-yl)-2,1,3-benzothiadiazole **3**. Compound **3** was then brominated in high yield to give 4,7-bis(7-bromo-9,9-dihexylfluoren-2-yl)-2,1,3-benzothiadiazole **4**, which was further modified *via* another Suzuki-coupling reaction with 4-(hydroxymethyl)phenylboronic acid pinacol ester to give product **5**. Finally, compound **5** was reacted with cinnamoyl chloride to afford the cinnamate-functionalised green emitter material 4,7-bis(7-(4-cinnamoyloxymethylphenyl)-9,9-dihexylfluoren-2-yl)-2,1,3-benzothiadiazole (**GreenCin**, **6**) in a high yield of 96% for the two final steps of the conversion of **4** to **6**.

**Synthesis of 4,7-bis(7-(4-oxymethylphenyl)-9,9-dihexylfluoren-2-yl)-2,1,3-benzothiadiazole (5)**

Deionised water (1.66 ml) was added to a mixture of the 4,7-bis(7-bromo-9,9-dihexylfluoren-2-yl)-2,1,3-benzothiadiazole (**4**) (0.3 g, 0.31 mmol), tetrakis(triphenyl phosphine)palladium (0) (0.07 g, 0.06 mmol), 4-(hydroxymethyl)phenyl boronic acid pinacol ester (0.22 g, 0.94 mmol), $Ba(OH)_2{\cdot}8H_2O$ (0.79 g, 2.5 mmol) in 30 ml tetrahydrofuran (THF), and the reaction mixture was degassed and stirred at 80 °C for 20 h. After aqueous work-up with $CH_2Cl_2$ and deionised water, the crude product was subjected to column chromatography on silica gel, eluting with toluene : ethyl acetate (10 : 1). The main fraction was precipitated from $CH_2Cl_2$–methanol, which afforded the product as a yellow-orange solid (97% yield). M.p. 101–104 °C.

MALDI TOF MS (dithranol as a matrix): *m*/*z* 1012.22 ($M^+$), 995.22 ($[M - OH]^+$).

Anal. Calcd for $C_{70}H_{80}N_2O_2S$: C, 82.96; H, 7.96; N, 2.76; found: C, 82.95; H, 7.65; N, 2.72.

$^1$H NMR (CDCl3, $\delta_H$, 400 MHz), 8.05 (2H, dd, $^3J$ = 7.9 Hz, $^4J$ = 1.6 Hz), 7.99 (2H, d, $^4J$ = 1.2 Hz), 7.91 (2H, s), 7.90 (2H, d, $^3J$ = 8.0 Hz), 7.84 (2H, d, $^3J$ = 7.8 Hz), 7.70 (4H, d, $^3J$ = 8.2 Hz), 7.62 (2H, dd, $^3J$ = 7.8 Hz, $^4J$ = 1.6 Hz), 7.60 (2H, s), 7.50 (4H, d, $^3J$ = 8.3 Hz), 4.79 (4H, d, $^3J$ = 5.9 Hz), 2.22–1.96 (8H, m), 1.67 (2H, t, $^3J$ = 6.0 Hz), 1.26–0.99 (24H, m), 0.95–0.73 (8H, m), 0.77 (12H, t, $^3J$ = 6.9 Hz).

$^{13}$C NMR ($CDCl_3$, $\delta_C$, 100 MHz), 154.5, 152.2, 151.6, 141.3, 141.1, 140.2, 140.1, 140.0, 136.4, 133.8, 128.4, 129.1, 127.7, 127.6, 126.2, 124.1, 121.7, 120.4, 120.0, 65.4, 55.5, 40.5, 31.6, 29.9, 24.1, 22.7, 14.2.

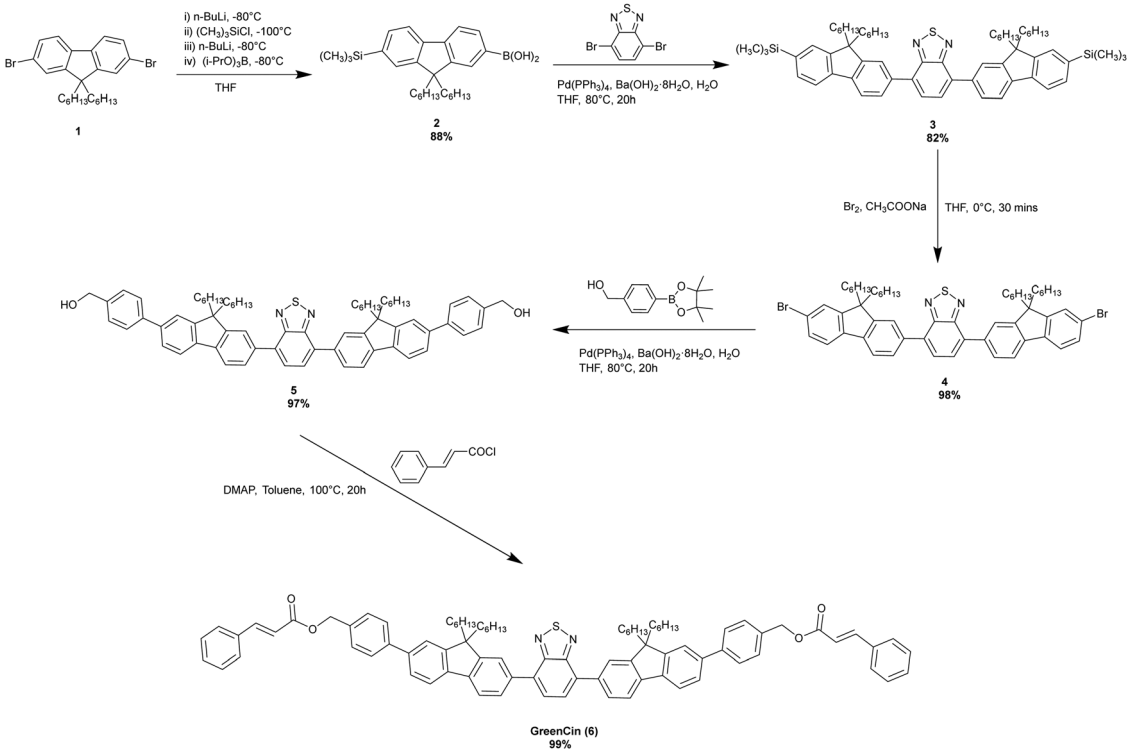


Scheme 1 The synthesis of **GreenCin**.

**Synthesis of 4,7-bis(7-(4-cinnamoyloxymethylphenyl)-9,9-dihexylfluoren-2-yl)-2,1,3-benzothiadiazole (GreenCin, 6)**

Cinnamoyl chloride (22.6 mg, 0.135 mmol) was added to a mixture of 4,7-bis(7-(4-oxymethylphenyl)-9,9-dihexylfluoren-2-yl)-2,1,3-benzothiadiazole (**5**) (45.9 mg, 0.045 mmol) and 4-dimethylaminopyridine (16.6 mg, 0.136 mmol) in 20 ml of dry toluene. The reaction mixture appeared as a milky suspension with white flakes formed and this was degassed and stirred at 100 °C for 20 h. After filtration and removal of the solvent, the crude product was purified by column chromatography on silica gel, eluting with $CH_2Cl_2$: petroleum ether 40–60 °C (1 : 1). Precipitation of the main fraction from $CH_2Cl_2$: methanol afforded a yellow-orange solid in 99% yield. M.p. 106–107 °C.

MALDI-TOF MS (retinoic acid as a matrix): $m/z$ – 1272.38 ($M^+$).

Anal. calcd for $C_{88}H_{92}N_2O_4S$: C, 82.98; H, 7.28; N, 2.20; found: C, 82.99; H, 7.24; N, 2.26.

$^1$H NMR ($CDCl_3$, $\delta_H$, 400 MHz) 8.05 (2H, dd, $^3J$ = 7.9 Hz, $^4J$ = 1.6 Hz), 7.99 (2H, d, $^4J$ = 1.2 Hz), 7.91 (2H, s), 7.90 (2H, d, $^3J$ = 7.6 Hz), 7.84 (2H, d, $^3J$ = 7.8 Hz), 7.77 (2H, d, $^3J$ = 16.0 Hz), 7.72 (4H, d, $^3J$ = 8.3 Hz), 7.62 (2H, dd, $^3J$ = 7.8 Hz, $^4J$ = 1.6 Hz), 7.60 (2H, s), 7.58–7.52 (8H, m), 7.45–7.35 (6H, m), 6.52 (2H, d, $^3J$ = 16 Hz), 5.33 (4H,s), 2.2–2.0 (8H, m), 1.2–1.0 (24H, m), 0.9–0.7 (8H, m), 0.77 (12H, t, $^3J$ = 6.9 Hz).

$^{13}$C NMR ($CDCl_3$, $\delta_C$, 101 MHz) 167.0, 154.5, 152.2, 151.6, 145.4, 141.9, 141.1, 140.3, 139.9, 136.4, 135.1, 134.5, 133.7, 130.5, 129.1, 128.4, 128.3, 128.1, 127.6, 126.3, 124.1, 121.8, 120.4, 120.0, 118.1, 66.3, 55.5, 40.5, 31.6, 29.9, 24.1, 22.7, 14.2.

# 3. Results and discussion

## 3.1 Optical characterisation of GreenCin

It is essential to fully understand the optical properties of organic emissive materials to evaluate their performance as down-converters. UV-Vis absorption spectroscopy measurements of samples in solid-state as well as their photoluminescence properties were studied. The solid-state measurements were performed on films that were prepared by spin-coating toluene solutions of 2.5 mg ml$^{-1}$ concentration of **GreenCin** on quartz substrates at 2000 rpm spin-speed.

The UV-Vis spectrum of **GreenCin** shows three major absorption peaks as seen in Fig. 2 for solution and solid-state measurements. The peak around 280 nm can be assigned to the cinnamoyl groups. The narrow peak around 335 nm corresponds to the π–π* transition of the fluorene arms whereas the broad peak around 430 nm corresponds to the intramolecular charge transfer (ICT) band. The absorption spectrum of **GreenCin** in the solid film is very similar to that in solution, but with a bathochromic shift (red shift) of 14 nm observed for the ICT band. This shift is likely to be due to dipole–dipole interactions of the molecules in the condensed phase. A similar bathochromic shift has been observed for a different linear quaterfluorene-DPP system.[38] The emission spectra in the film are blue-shifted by 11 nm compared to the emission spectra in $CH_2Cl_2$, due to a lower degree of excited state structural relaxation before emission in the condensed phase. The results of

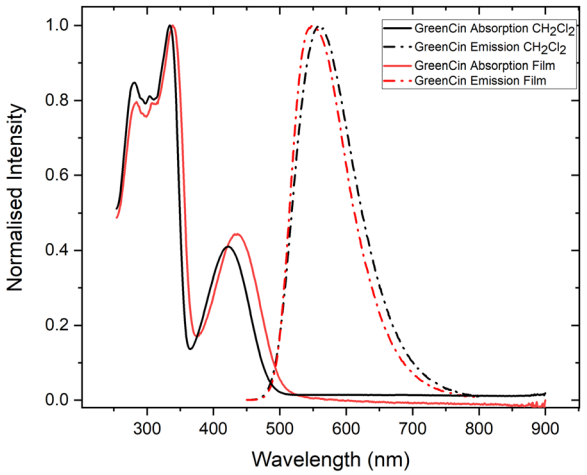


Fig. 2 Normalised UV-Vis absorption (solid lines) and emission spectra (dashed lines) of **GreenCin** measured in $CH_2Cl_2$ solution (black lines) and in the solid state (red line). Both solution and solid films were excited at 421 nm.

solution and solid state measurements are summarised in Table 1. The optical properties of **GreenCin** are suitable for an energy down-converter for blue light as the main absorption band at 436 nm in the solid-state is close to the wavelength of blue light emitted by most commercially used blue LEDs, which typically emit near 450 nm. Additionally, the PLQY value for **GreenCin** in the solid state is 84% which makes it an excellent light-emitting organic dye and can consequently increase the down-converting performance.

## 3.2 Photoreactive properties

The photoreactive properties of **GreenCin** and the cross-linking process between **GreenCin** and **TCM** were examined by treating the samples with UV irradiation. The samples were prepared by spin-coating the target solutions on quartz substrates at 2000 rpm. The process was monitored by UV-Vis absorption spectroscopy measurements.

Initially, the photoreactive properties of the monomer **TCM** as a single component were studied. Fig. 3(a) shows the changes in the UV-vis absorption spectra of **TCM** film after exposure to 254 nm UV light over a time span of 90 minutes. The peak at 294 nm corresponds to the absorption of the cinnamate moieties. The peak decreases upon further irradiation and disappears after 90 min, which indicates that the cross-linking process between cinnamate groups by a

Table 1 Summary of the optical properties of GreenCin in $CH_2Cl_2$ and in the solid state (film)

| $\lambda_{max}^{abs}$ in $CH_2Cl_2$[a] [nm] | $\lambda_{max}^{em}$ in $CH_2Cl_2$[b] [nm] | PLQY in $CH_2Cl_2$[cd] [%] | $\lambda_{max}^{abs}$ film [nm] | $\lambda_{max}^{em}$ film[e] [nm] | PLQY film[c] [%] |
|---|---|---|---|---|---|
| 280, 334, 422 | 560 | 94 | 284, 339, 436 | 549 | 84 |

[a] Recorded in $CH_2Cl_2$ at $10^{-5}$ M. [b] Recorded in $CH_2Cl_2$ at $10^{-6}$ M with excitation at 421 nm. [c] Absolute values. [d] Recorded in $CH_2Cl_2$ at $10^{-6}$ M. [e] Excitation at 421 nm.

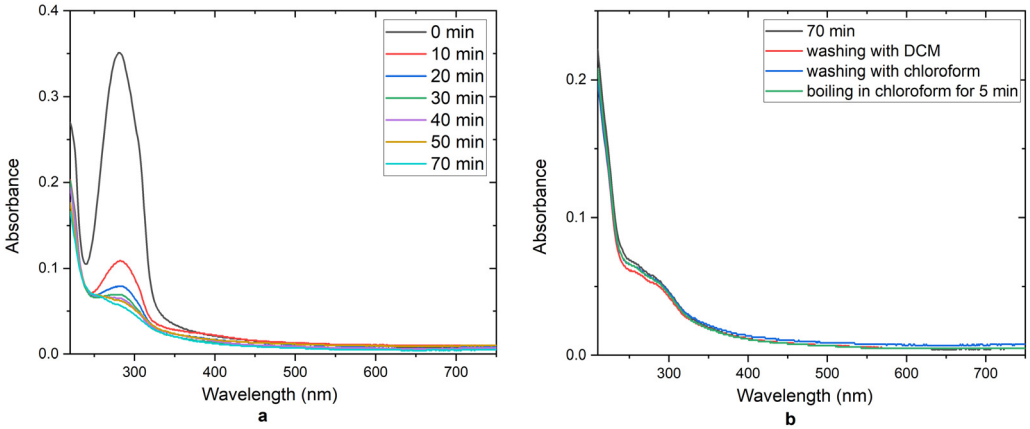


Fig. 3 (a) UV-Vis absorption spectra as a function of UV exposure time that verify the cross-linking process of **TCM**; (b) the resulting film was subjected to washing steps that indicate the insolubility of the cross-linked polymer system.

cycloaddition is complete. In order to test the stability of films when in contact with solvents, the film was rinsed with $CH_2Cl_2$, followed by rinsing with chloroform, and finally immersion in hot chloroform for 5 minutes. The UV-Vis spectra were measured after each washing stage (Fig. 3(b)). The results showed no change in the absorption spectra which indicates the insolubility of the cross-linked **TCM** matrix.

For comparison, the photocycloaddition processes of the **GreenCin** monomer were studied by the same method. The resulting polymer structure, **p(GC)**, is shown in Fig. 4(a). Fig. 4(b) shows a similar change in the cinnamate absorption band where the intensity of the peak at 291 nm diminished, indicating the completion of polymerisation between **GreenCin** molecules. However, the films of **p(GC)** were completely washed-off upon rinsing with $CH_2Cl_2$, which proved that the linear polymer of **GreenCin** created upon UV-irradiation (with a molecular weight of 12.0 kDa), has good solubility.

To study the cross-linking ability of **TCM**, stock solutions of the same concentration of **TCM** and **GreenCin** in toluene were prepared (2 mM) separately. The ratio between **GreenCin** and **TCM** was kept at 1 : 10 in order to have a high degree of cross-linking between these two materials without sacrificing the down-converting efficiency due to the solution being too diluted. Fig. 5 shows the idealised structure of the cross-linked copolymer between **GreenCin** and **TCM**.

The cross-linking process was monitored by performing UV-vis spectroscopy measurements of films at intervals of 20 min. Fig. 6(a) shows the UV-vis absorption spectra of the cross-linking process. The intensity for the absorption of the cinnamate groups (291 nm) was significantly higher than that for the previous samples as additional cinnamate groups were introduced when mixing **TCM** with **GreenCin**. After no further reduction in the cinnamate peak could be observed from the UV-Vis spectra, the samples were rinsed with $CH_2Cl_2$, which washed off any unreacted materials and by-products such as linear **GreenCin** polymer and co-polymers of **TCM-GreenCin** with low molecular weight. This explains the decrease in absorption across the entire spectra after the first wash. The remaining

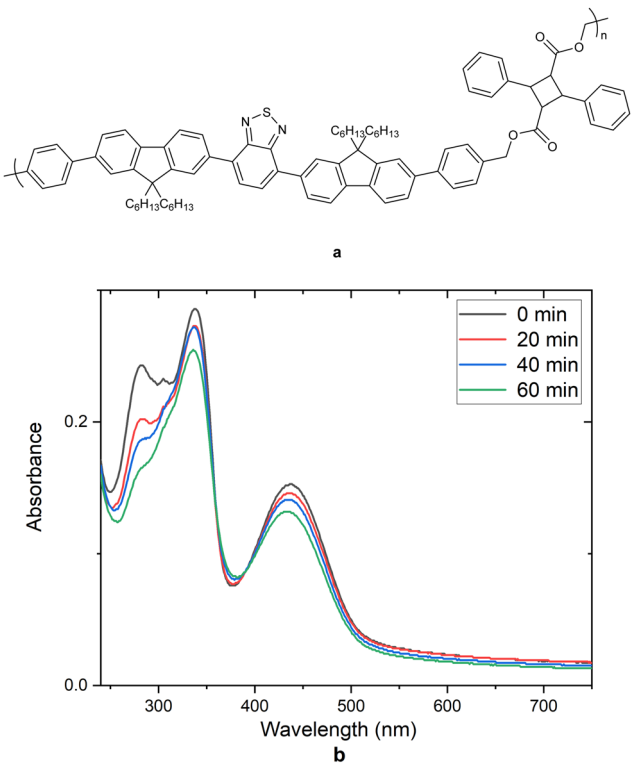


Fig. 4 (a) Chemical structure of linear polymer **p(GC),** and (b) absolute UV-Vis absorption spectra that demonstrate the polymerisation process where the 291 nm peak diminished towards the completion of polymerisation.

film was then proven to be insoluble after washing with chloroform and then immersing in hot chloroform for 5 min with no change in absorption intensity (Fig. 6(b)). These data confirm the successful cross-linking between **GreenCin** and **TCM**.

The PLQY values of films obtained from **GreenCin** and **TCM** composite material were also studied in thick (drop-cast) and thin (spin-coated) films. The films were prepared by three different ways: spin-coated and not cross-linked; spin-coated,

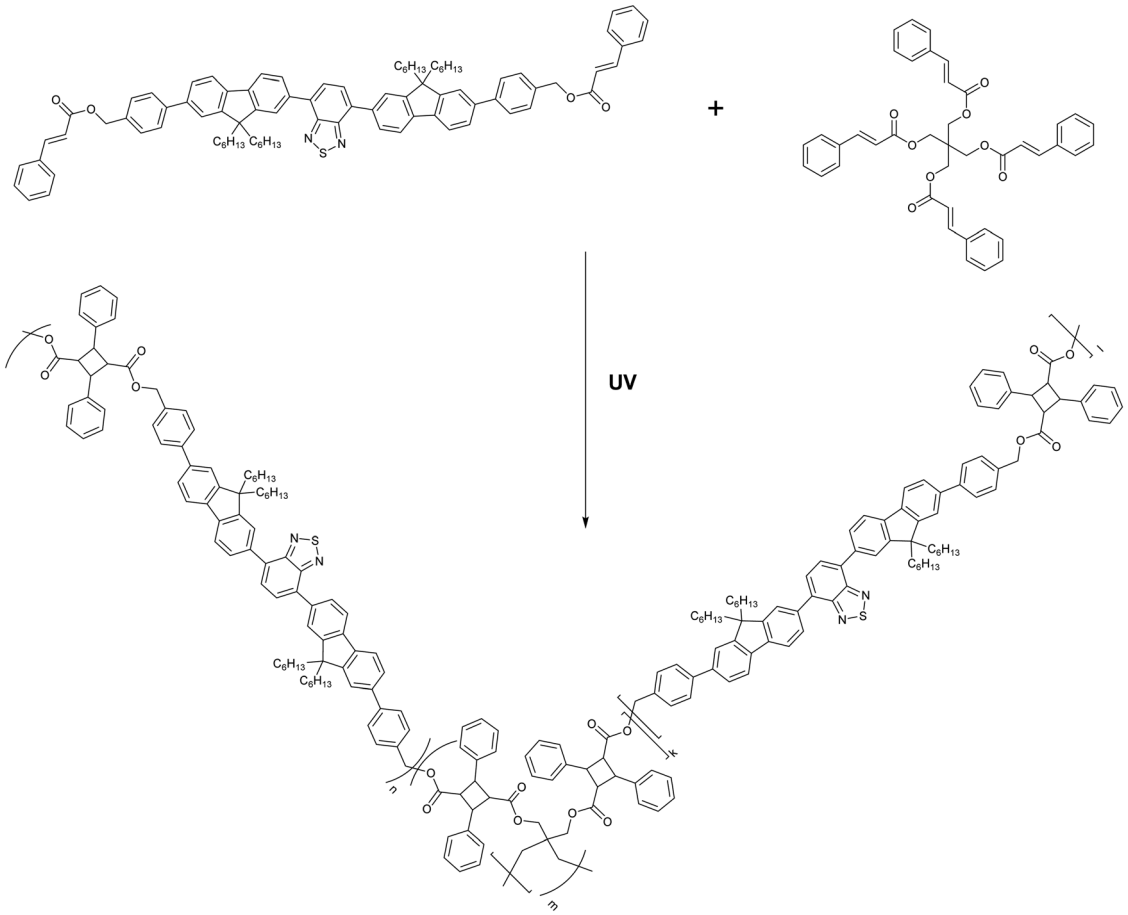


Fig. 5 Idealised structure of the product of polymerisation between **GreenCin** and **TCM**. The repeating units in 'curly' brackets and 'square' brackets represent statistical polymer chains in different directions of the cross-linked polymer.

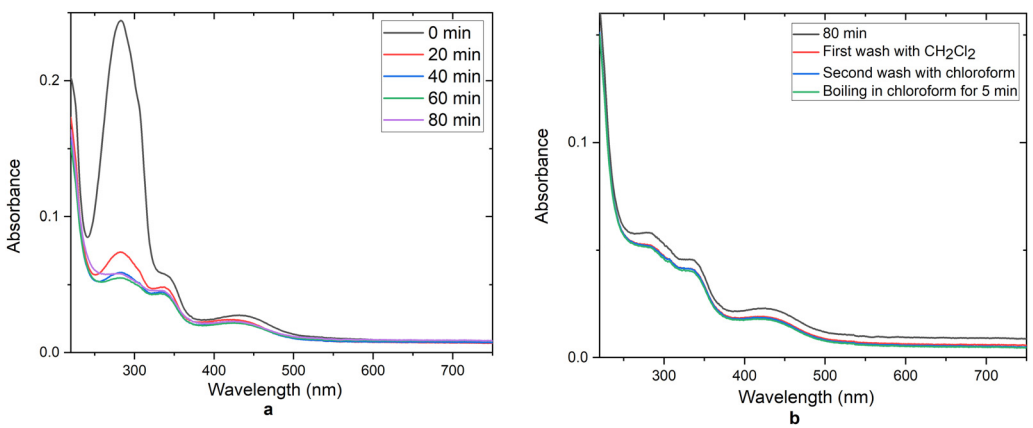


Fig. 6 (a) UV-Vis absorption spectra as a function of UV exposure time verifying the cross-linking process between **GreenCin** and **TCM**; (b) UV-Vis absorption spectra of the resulting film subjected to washing steps that indicate the insolubility of the cross-linked polymer system.

cross-linked and washed with $CH_2Cl_2$; drop-casted, cross-linked and washed with $CH_2Cl_2$. The summary of PLQY values and PLQY spectrum are shown in Table 2 and Fig. 7. It can be seen that the PLQY values of films that were prepared by spin-coating were significantly lower than the films that were prepared by drop-casting. The reason for this was mainly due to the small quantity of emissive material remaining on the resulting films following the spin-coating process. However, since the deposition method used to fabricate hybrid devices was by drop-casting (details of device fabrication is discussed in

 

Table 2 Summary of PLQY studies of GreenCin 1 : 10 TCM films

| Deposition method/treatments | PLQY (%) |
|---|---|
| Spin-coated, no cross-linking or washing | 19 |
| Spin-coated, cross-linked and washed with $CH_2Cl_2$ | 11 |
| Drop-cast, cross-linked and washed with $CH_2Cl_2$ | 87 |

the next section), the amounts of emissive materials remaining on the blue LEDs were higher. Thus, the PLQY value obtained from this method shows more relevance and was also consistent with the PLQY value determined for the neat GreenCin films.

### 3.3 Down-converting device properties

The blue-emitting InGaN/GaN LEDs used for this work were manufactured by Plessey Semiconductors Ltd. The LEDs emit near 450 nm, which has good overlap with the absorption peak of **GreenCin** at 436 nm in the solid state. Thus, the emitted blue light from the inorganic LEDs can be absorbed and down-converted by the organic layer. **GreenCin** and **TCM** (1 : 10 molar ratio) were dissolved in tetrahydrofuran at a concentration of 16 mg $ml^{-1}$ for the emitter material. The solution was drop-cast onto a blue LED and cross-linked under 254 nm UV irradiation to form a green-emitting film on the top. However, due to the presence of two cinnamate-functionalised materials, self-polymerisation of **GreenCin** and short-chain copolymers of **TCM** and **GreenCin** can also be created. Therefore, the down-converting layer was washed with $CH_2Cl_2$ to remove any materials before a second layer of cross-linked **TCM** film was applied on the top of the down-converting film to protect it from the ambient environment which contains oxygen and water. The deposition process and an image of the hybrid LED under operation inside the integrating sphere are shown in Fig. S1 in the ESI.†

Fig. 8 shows the electroluminescence (EL) spectra of hybrid devices that were measured under a constant current of 25 mA inside an integrating sphere. Device 1 to 8 follow the trend of increasing amount of **GreenCin–TCM** solution drop-cast onto the blue LEDs that were later cross-linked under UV to yield films with increasing emission intensities. Fig. 8(a) shows the absolute EL spectra whereas the green-emission peaks are normalised against the blue-emission peaks in Fig. 8(b) so that the difference of intensities can be seen more easily. Two distinct emission peaks were observed in both spectra. The emission peak at 450 nm can be assigned to the blue LED whereas the emission peak at 540 nm can be assigned to the green-emission from the cross-linked copolymer films. With the increase of the amount of down-converting material, the intensity of green emission increases. As a result, the ratio

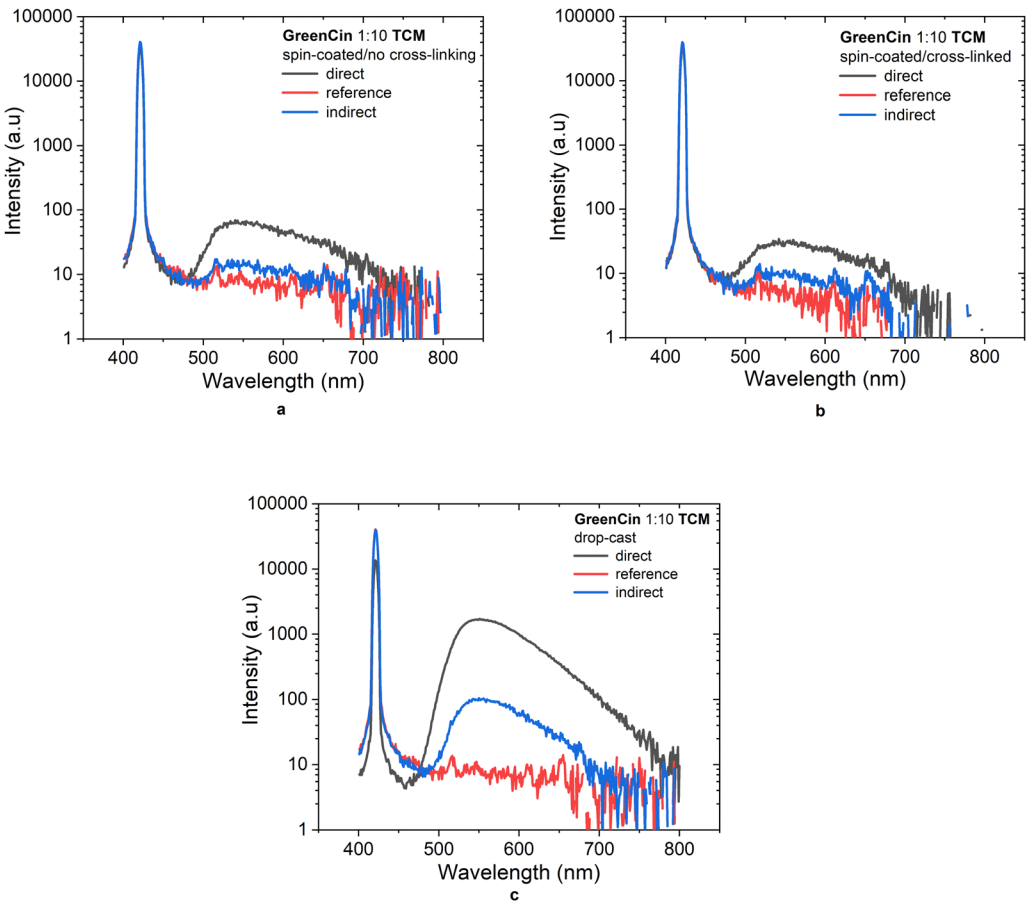


Fig. 7 Direct, indirect and reference plots for spin-coated films deposited using 1 : 10 GreenCin to TCM mixture (a) with no cross-linking, (b) subjected to UV cross-linking and washing with $CH_2Cl_2$ and (c) drop-casted films that were subjected to UV cross-linking and washing with $CH_2Cl_2$.

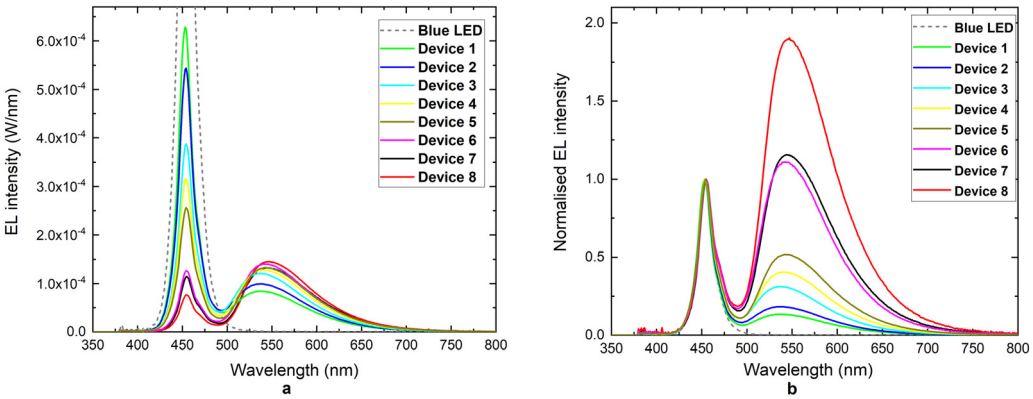


Fig. 8 (a) Absolute EL spectra taken at 25 mA from device 1 (lowest **GreenCin** load) to device 8 (highest **GreenCin** load) which indicate that good green emission can be achieved overall with increasing **GreenCin** load; (b) normalised EL spectra from device 1 to device 8 which indicate that the ratio between the green-emission peak and the blue-emission peak increases with the increase of the amount of **GreenCin** material deposited on LEDs, thus better down-converting performance can be achieved.

between green emission and blue emission increases. Thus, a higher yield of blue light being absorbed and converted by the organic material can be achieved.

White light emission was confirmed by CIE 1931 chromaticity coordinates, which were calculated from the EL spectra. Several hybrid devices with different green-emission intensity were made and their chromaticity coordinates are shown in the CIE 1931 plot (Fig. 9). Chromaticity coordinates of a bare blue LED and **GreenCin** were also included as a reference. It can be seen that the data points form a line that cuts through the Planckian locus from the near blue region to near green region, with some lying near the region of ideal white light emission.

In addition to the chromaticity coordinates, correlated colour temperature (CCT) can also be used to quantify the colour of the emission. The CCT value can be calculated by determining the shortest distance between the chromaticity point and the Planckian locus.[39] It is also often used to categorise a white light as 'cool white' or 'warm white'. The CCT values for the emissions of hybrid devices that lie in the cool-white region and warm-white region are 7490 K and 4750 K respectively, which covers the colour region between cool and warm white light. Therefore, colour tuning of white light emission from the hybrid devices can be achieved by varying the amount of organic materials coated on blue LEDs. The fidelity and the quality of the white light emission can be described by the colour rendering index (CRI), which ranges between 0 to 100 with the maximum value representing an ''ideal'' colour rendering source such as an incandescent light bulb.[7] The CRI values for the hybrid devices range between 52 and 69, which is reasonable for hybrid devices with only one organic down-converting material, and are similar to the colour rendering ability achieved with similar organic down-converting materials that consist of BT-fluorene core structures.[33] Overall, the CRI value reduces as the green emission intensity increases. This indicates that high colour rendering quality is achieved with cool white light. The biggest contribution to the good colour-rendering ability is the low self-absorption of the organic material.

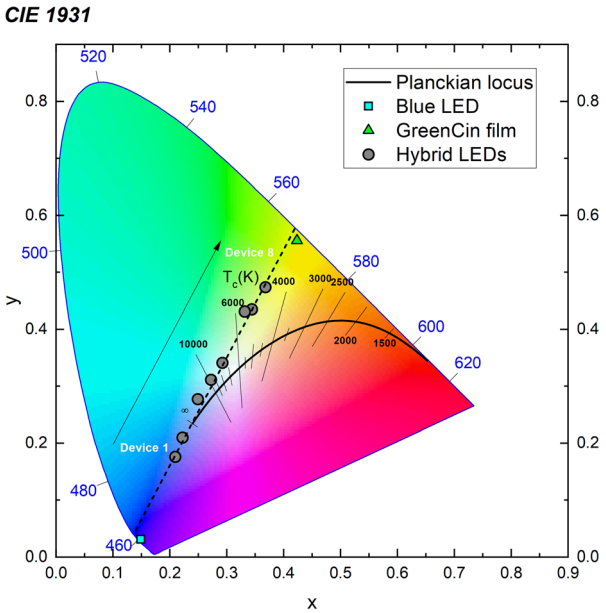


Fig. 9 CIE 1931 chromaticity diagram of hybrid devices showing the relationship between the colour coordinates and the amount of **GreenCin** coated on LEDs. Arrow indicates direction of increasing **GreenCin** load.

Apart from the characterisation of light produced by the hybrid devices, additional parameters are used to quantify the down-converting efficiencies of the organic materials in the hybrid devices. Radiant flux (W) can be used to determine the optical power of the device whilst luminous efficacy (lm $W^{-1}$) can be used to determine the ability of a device to convert electrical power to light. It is worth mentioning that luminous efficacy is defined by the ratio of luminous flux and the input electric power, whilst taking into account how the human eye responds to visible light, whereas radiant flux only considers the optical performance of devices without considering how the human eye perceives the light.[25,39] Table 3 shows the luminous efficacy values for the hybrid devices with different green emission intensities (different amounts of organic materials coated on blue LEDs). The luminous efficacy value increases with the

 

Table 3 Summary of the down-converting properties of hybrid devices. Device 1 has the lowest amount of **GreenCin** coated on the blue LED, whereas device 8 has the highest amount of **GreenCin** coated on the blue LED

| Hybrid device | Luminous efficacy (lm $W^{-1}$) | Radiant flux (mW) | Blue-to-white efficacy (lm $W^{-1}$) |
|---|---|---|---|
| Device 1 | 71.3 | 24.0 | 138 |
| Device 2 | 81.9 | 23.8 | 162 |
| Device 3 | 94.6 | 22.0 | 197 |
| Device 4 | 99.0 | 16.5 | 193 |
| Device 5 | 110.6 | 21.2 | 185 |
| Device 6 | 103.4 | 20.3 | 205 |
| Device 7 | 104.1 | 17.4 | 213 |
| Device 8 | 107.1 | 16.5 | 212 |

increase of green emission intensity. The highest luminous efficacy value achieved with this type of hybrid device is 107 lm $W^{-1}$. By comparison, this is more than 2 times higher than the last generation of organic down-converting materials that utilise similar BT-fluorene core structures.[33] The high luminous efficacy can be explained by the high PLQY value of 84% in the solid-state. The radiant flux values for hybrid devices decrease with increased green emission intensity (from cool to warm white light), with the highest value being 24 mW. In addition, blue-to-white efficacy can be used as a supplementary parameter to further describe the down-converting efficiency. The term is defined by the ratio of the luminous flux (lm) of the hybrid devices with the radiant flux of the bare blue LED (W).[3] This can further illustrate how much of the emitted blue light from the LED is converted to white light by down-converting materials.[39] The blue-to-white efficacy values follow a similar trend to the values of luminous efficacy, where the value increases with the increase of green emission intensity. The highest blue-to-white efficacy value is 213 lm $W^{-1}$ (device 7).

It is worth mentioning that this new generation of organic down-converting material based on the BT-fluorene core structure shows some improvements when compared to the similar green-emitter material, $(TPA\text{-}Flu)_2BT$.[33] Table 4 shows some of the key values that were used to compare the down-converting ability of this organic material. In general, **GreenCin** has a higher PLQY value, higher luminous efficacy and higher radiant flux values, and a similar CRI range when compared to $(TPA\text{-}Flu)_2$-BT. However, the only drawback of this new material based on the measurements is the lower blue-to-white efficacy value with comparison to the $(TPA\text{-}Flu)_2BT$. This might be caused by the area coverage differences between dome-shaped CHDV membranes that contain $(TPA\text{-}Flu)_2BT$ and the thin films of cross-linked **TCM-GreenCin** copolymer. Due to the small volume of **GreenCin** solution that was deposited on the blue LEDs, the material tends to accumulate around the LED edge or wire bonds, which is a common problem for direct deposition of organic dyes on LEDs.[40] Thus, fewer blue photons were absorbed and down-converted by **GreenCin** molecules. The blue-to-white efficacy value can be improved either by tuning the optical properties of the **GreenCin** material to shift its absorption band to more closely match the wavelength of commercially used blue LEDs (450 nm) or by physically increasing the area coverage of organic down-converting materials on the LEDs. Of strategic importance, an increase in the number of incoming blue photons absorbed will lead to a higher blue-to-white efficacy.

Table 4 Summary of key values that determine the down-converting efficiencies of **GreenCin**, and **$(TPA\text{-}Flu)_2BT$**

| Material | PLQY | Luminous efficacy (lm $W^{-1}$) | Radiant flux (mW) | Blue-to-white efficacy (lm $W^{-1}$) | CRI |
|---|---|---|---|---|---|
| **GreenCin** | 84% | 107 | 24 | 213 | 52–69 |
| **$(TPA\text{-}Flu)_2BT$** | 61% | 41 | 10.2 | 368 | 51–66 |

### 3.4 Stability study of GreenCin

Measuring the high performance of organic materials as down-converting layers for inorganic LEDs is important. However, organic materials can suffer from poor thermal or photo-stability and this limits the lifetime of hybrid devices. Ideally, cross-linked polymers are more stable than their monomers. Thermodynamically, the total energy of the monomers combined is higher than the total energy of the polymers.[24] Mechanically, due to the entanglements of polymer chains, cross-linked polymers tend to have restricted chain movements which lead to lower degree of freedom and hence, higher stability.[41] Therefore, **GreenCin** in its matrix form should be relatively more stable than other non-cross-linkable organic down-converting monomers.

The degradation of the hybrid devices was studied by recording the devices' EL spectra regularly over several months to check if there was any significant decrease of the green-emission peak as well as a change in chromaticity coordinates. Initial measurements of the early batches of hybrid devices showed a decrease in the green-emission peak (data not shown) and was suspected to be caused by photo-oxidation due to the organic layers being in contact with the atmosphere. Protection of the organic layer was attempted by adding an additional layer such as a poly(CHDV) membrane or a **TCM** film as encapsulant. However, the green emission continued to decrease over several weeks of time whilst the chromaticity coordinates shifted towards the blue region.

It was later realised that the stability issue could potentially be caused by another polymer material in the organic layer. As mentioned above, the cross-linked organic down-converting layer was prepared by reacting **GreenCin** and **TCM** monomers to form a matrix system. However, **GreenCin** being a cinnamate-functionalised material also has the tendency to self-polymerise to form a linear polymer system (p(GC)) and short-chained copolymer of **TCM** and **GreenCin**. These unwanted polymer materials are soluble in most organic solvents whereas the cross-linked polymer is not. After the down-converting material was treated with UV irradiation, the organic layer was washed with $CH_2Cl_2$ to wash off the residual unreacted monomers and short-chain polymers. The EL spectra of one of the best performing hybrid devices is promising (device 6). The hybrid LED was studied by driving the LED for

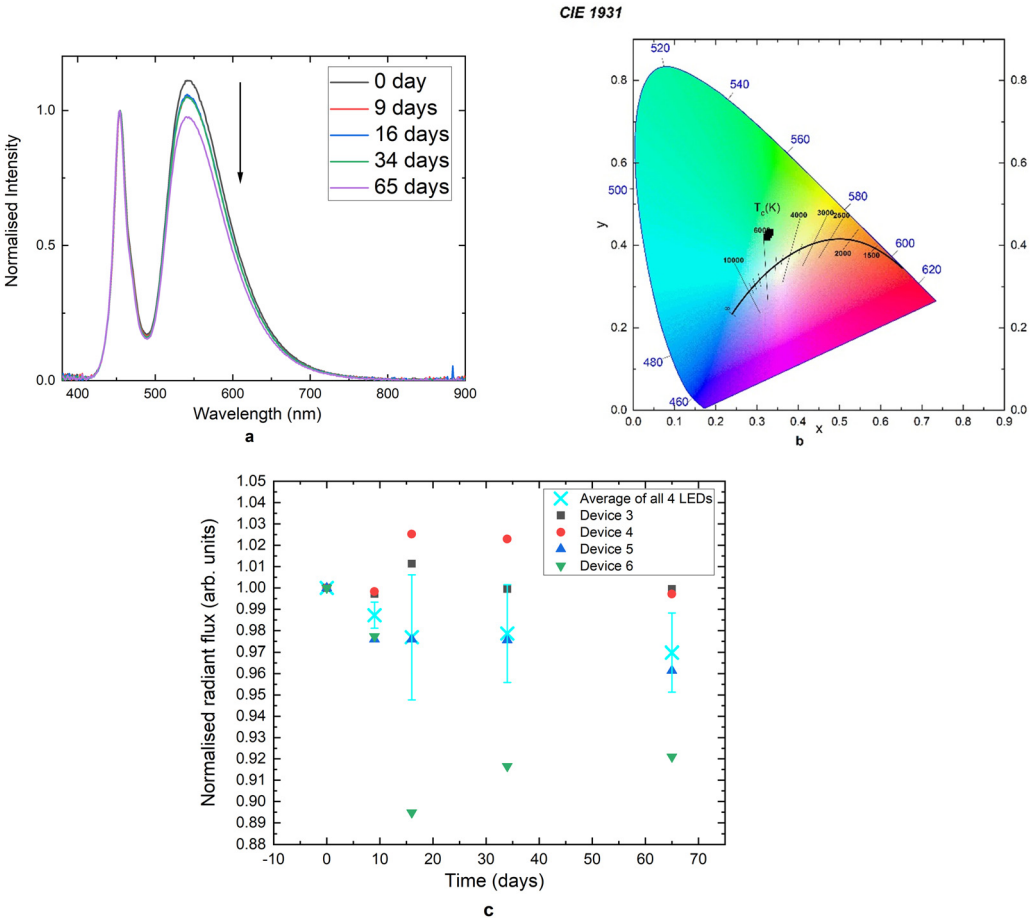


Fig. 10 (a) EL spectra of the degradation process of device 6. The arrow indicates the direction of decreasing green-emission throughout the measurements; (b) CIE 1931 chromaticity diagram of device 6 indicating very minimal changes in coordinates; (c) plot of normalised radiant flux against time for four hybrid devices (each hybrid device is normalised to their initial radiant flux value at time zero) and the average values of all four hybrid devices that indicate a small degree of degradation.

a short period of time under a constant current of 25 mA at different time intervals over a time-span of 65 days. The green-emission peaks were normalised against the blue emission peak (Fig. 10(a)). Initially, there was a drop in the green emission intensity during the second measurement that was conducted 9 days after the initial measurement. The degradation could be caused by the residue of small molecules/polymers in the system that were not successfully removed. The organic down-converting material stabilised after the first week and no further change was observed during subsequent measurements that were conducted after 34 days. However, the green emission decreased after the 5th measurement that was performed 65 days after the device was made, although the scale of the degradation is rather minimal. Table 5 lists all the key parameters across the 5 measurements. It can be seen that throughout the measurements, radiant flux, luminous flux, CRI and luminous efficacy values remained basically the same, with small changes in CCT and blue-to-white efficacy ratio. The small degree of change can be further illustrated by the CIE 1931 chromaticity diagram where all the data points lie near the same region with little change in coordinates (Fig. 10(b)). It is worth mentioning that the films that were deposited on LEDs showed relatively good stability when compared to other down-converting materials that were embedded in polymer matrix systems such as poly(CHDV) and poly(urethane) membranes.[25,26]

Table 5 Summary of key parameters obtained from 5 measurements during the degradation study for device 6

| Measurements | Time (days) | Radiant flux (mW) | Luminous flux (lm) | CCT (K) | CRI | Luminous efficacy (lm $W^{-1}$) | Blue-to-white ratio (lm $W^{-1}$) |
|---|---|---|---|---|---|---|---|
| 1st | 0 | 17.4 | 7.0 | 5536 | 55.0 | 104.1 | 213.4 |
| 2nd | 9 | 17.4 | 6.9 | 5628 | 55.2 | 103.7 | 210.2 |
| 3rd | 16 | 17.9 | 7.1 | 5612 | 55.0 | 107.3 | 218.2 |
| 4th | 34 | 17.8 | 7.1 | 5633 | 55.1 | 107.1 | 217.5 |
| 5th | 65 | 17.4 | 6.9 | 5759 | 55.5 | 103.2 | 209.7 |

A similar degradation pattern can also be seen from the other hybrid devices. Fig. 10(c) shows the plot of radiant flux against time for 4 hybrid devices with each device's radiant flux value normalised to its initial value. The average values for all 4 hybrid devices are also included.

## 4. Conclusions

In this work we have reported the synthesis, characterisation and fabrication of hybrid devices for white light emission with a novel organic down-converting material, **GreenCin**. This green-emitting material can produce good quality white light when incorporated with inorganic InGaN/GaN blue LEDs due to its favourable optical properties such as high PLQY (94% in $CH_2Cl_2$ and 84% in the solid state) compared to the last generation of down-converting organic materials. The functionalisation of the material with cinnamate groups allows the cross-linking reaction between **GreenCin** with **TCM** to form a physically stable film. Thus, no additional host matrix material such as poly(CHDV) or poly(urethane) is needed for the encapsulation of organic materials. Using this new approach, photoacid generators can be avoided in the cross-linking process, which can degrade the emissive organic emitter in the hybrid device. It has been shown that the resulting hybrid device can produce white light more efficiently than the last generation of green-emission organic materials based on similar chemical structures with 2.6 × luminous efficacy (107 lm $W^{-1}$), 2.4 × radiant flux (24 mW) and high blue-to-white efficacy (213 lm $W^{-1}$). Colour tuning can also be achieved with the hybrid device by varying the amount of **GreenCin** that was deposited on blue LEDs that leads to 'cool' to 'warm' white light emission. The quality of the white light produced by hybrid devices also proved to be reasonable with a CRI value range between 52–69 with values above 80 being the target for viable white sources. Although some degradation of the down-converting layer was observed during the lifetime measurements, the decrease in emission in the green region was minimal, even when compared to some other down-converting materials that were encapsulated in additional host matrix materials. Despite the green emission decreasing gradually throughout the measurements, both radiant flux and luminous flux remain relatively stable, whilst the luminous efficacy and blue-to-white ratio did not fluctuate drastically. Therefore, we have reported a new approach to creating white light emitting hybrid LEDs, with a new class of photopolymerisable materials used for LEDs with high performance and good stability.

## Conflicts of interest

There are no conflicts to declare.

## Acknowledgements

The authors thank EPSRC for funding through grants EP/P02744X/2 and EP/R03480X/1. DJW acknowledges support from EPSRC fellowship (EP/N01202X/2).

## References

1 K. T. Kamtekar, A. P. Monkman and M. R. Bryce, *Adv. Mater.*, 2010, **22**, 572–582.
2 J. Bruckbauer, C. Brasser, N. J. Findlay, P. R. Edwards, D. J. Wallis, P. J. Skabara and R. W. Martin, *J. Phys. D: Appl. Phys.*, 2016, **49**, 405103.
3 J. Bruckbauer and N. J. Findlay, in *Optoelectronic Organic-Inorganic Semiconductor Heterojunctions*, ed. Y. Zhou, CRC Press, Boca Raton, 1st edn, 2021, ch. 10, pp.231–266.
4 V. Anand, R. Mishra and Y. Barot, *Dyes Pigm.*, 2021, **191**, 109390.
5 Y. Fu, P. Xiong, X. Liu, X. Wang, S. Wu, Q. Liu, M. Peng and Y. Chen, *J. Mater. Chem. C*, 2021, **9**, 303–312.
6 K. P. O'Donnell, M. Auf der Maur, A. Di Carlo, K. Lorenz and T. S. Consortium, *Phys. Status Solidi RRL*, 2012, **6**, 49–52.
7 C. J. Humphreys, *MRS Bull.*, 2011, **33**, 459–470.
8 C. R. Ronda, T. Jüstel and H. Nikol, *J. Alloys Compd.*, 1998, **275–277**, 669–676.
9 B. Lei, B. Li, H. Zhang and W. Li, *Opt. Mater.*, 2007, **29**, 1491–1494.
10 G. Li, Z. Wang, Z. Quan, C. Li and J. Lin, *Cryst. Growth Des.*, 2007, **7**, 1797–1802.
11 T.-C. Liu, B.-M. Cheng, S.-F. Hu and R.-S. Liu, *Chem. Mater.*, 2011, **23**, 3698–3705.
12 R. K. Tamrakar, D. P. Bisen, I. P. Sahu and N. Brahme, *J. Radiat. Res. Appl. Sci.*, 2014, **7**, 417–429.
13 M. Yu, J. Lin, Z. Wang, J. Fu, S. Wang, H. J. Zhang and Y. C. Han, *Chem. Mater.*, 2002, **14**, 2224–2231.
14 P. Schlotter, J. Baur, C. D. Hielscher, M. Kunzer, H. Obloh, R. Schmidt and J. Schneider, *Mater. Sci. Eng., B*, 1999, **59**, 390–394.
15 K. Bando, K. Sakano, Y. Noguchi and Y. Shimizu, *J. Light Visual Environ.*, 1998, **22**, 2–5.
16 H. Ju, W. Deng, B. Wang, J. Liu, X. Tao and S. Xu, *J. Alloys Compd.*, 2012, **516**, 153–156.
17 H. Zhu, C. C. Lin, W. Luo, S. Shu, Z. Liu, Y. Liu, J. Kong, E. Ma, Y. Cao, R.-S. Liu and X. Chen, *Nat. Commun.*, 2014, **5**, 4312.
18 Z. Yue, Y. F. Cheung, H. W. Choi, Z. Zhao, B. Z. Tang and K. S. Wong, *Opt. Mater. Express*, 2013, **3**, 1906–1911.
19 S. Massari and M. Ruberti, *Resour. Policy*, 2013, **38**, 36–43.
20 X. A. Cao, S. Li, X. M. Li and L. Y. Liu, *IEEE Trans. Electron Devices*, 2018, **65**, 4891–4896.
21 J. McKittrick, L. E. Shea-Rohwer and D. J. Green, *J. Am. Ceram. Soc.*, 2014, **97**, 1327–1352.
22 N. Muhamad Sarih, P. Myers, A. Slater, B. Slater, Z. Abdullah, H. A. Tajuddin and S. Maher, *Sci. Rep.*, 2019, **9**, 1–8.
23 Z. He, W. Zhao, J. W. Y. Lam, Q. Peng, H. Ma, G. Liang, Z. Shuai and B. Z. Tang, *Nat. Commun.*, 2017, **8**, 1–7.
24 M. Mosca, R. Macaluso and I. Crupi, in *Polymers for Light-Emitting Devices and Displays*, ed. I. Inamuddin, R. Boddula, M. I. Ahmed and A. M. Asiri, Wiley-Scrivener, Hoboken-Beverly, 2020, ch. 8, pp. 197–262.
25 A. A. Wiles, J. Bruckbauer, N. Mohammed, M. Cariello, J. Cameron, N. J. Findlay, E. Taylor-Shaw, D. J. Wallis, R. W. Martin, P. J. Skabara and G. Cooke, *Mater. Chem. Front.*, 2020, **4**, 1006–1012.

26 N. J. Findlay, J. Bruckbauer, A. R. Inigo, B. Breig, S. Arumugam, D. J. Wallis, R. W. Martin and P. J. Skabara, *Adv. Mater.*, 2014, **26**, 7290–7294.
27 R. Smith, B. Liu, J. Bai and T. Wang, *Nano Lett.*, 2013, **13**, 3042–3047.
28 G. Heliotis, P. N. Stavrinou, D. D. C. Bradley, E. Gu, C. Griffin, C. W. Jeon and M. D. Dawson, *Appl. Phys. Lett.*, 2005, **87**, 103505.
29 H. Chun, P. Manousiadis, S. Rajbhandari, D. A. Vithanage, G. Faulkner, D. Tsonev, J. J. D. McKendry, S. Videv, E. Xie, E. Gu, M. D. Dawson, H. Haas, G. A. Turnbull, I. D. W. Samuel and D. C. O'Brien, *IEEE Photonics Technol. Lett.*, 2014, **26**, 2035–2038.
30 F. Hide, P. Kozodoy, S. P. DenBaars and A. J. Heeger, *Appl. Phys. Lett.*, 1997, **70**, 2664–2666.
31 E. Aksoy, N. Demi̇r and C. Varlikli, *Can. J. Phys.*, 2018, **96**, 734–739.
32 C. Karapire, C. Timur and S. İçli, *Dyes Pigm.*, 2003, **56**, 135–143.
33 E. Taylor-Shaw, E. Angioni, N. J. Findlay, B. Breig, A. R. Inigo, J. Bruckbauer, D. J. Wallis, P. J. Skabara and R. W. Martin, *J. Mater. Chem. C*, 2016, **4**, 11499–11507.
34 C. R. Belton, A. L. Kanibolotsky, J. Kirkpatrick, C. Orofino, S. E. T. Elmasly, P. N. Stavrinou, P. J. Skabara and D. D. C. Bradley, *Adv. Funct. Mater.*, 2013, **23**, 2792–2804.
35 A. V. Rami Reddy, K. Subramanian and A. V. Sesha Sainath, *J. Appl. Polym. Sci.*, 1998, **70**, 2111–2120.
36 S. Y. Cho, J. G. Kim and C. M. Chung, *J. Nanosci. Nanotechnol.*, 2010, **10**, 6972–6976.
37 D. R. Coulson, L. C. Satek and S. O. Grim, *Inorg. Synth.*, 1972, pp.121–124.
38 A. L. Kanibolotsky, F. Vilela, J. C. Forgie, S. E. Elmasly, P. J. Skabara, K. Zhang, B. Tieke, J. McGurk, C. R. Belton, P. N. Stavrinou and D. D. Bradley, *Adv. Mater.*, 2011, **23**, 2093–2097.
39 E. Taylor, P. R. Edwards and R. W. Martin, *Phys. Status Solidi A*, 2012, **209**, 461–464.
40 N. J. Findlay, C. Orofino-Peña, J. Bruckbauer, S. E. T. Elmasly, S. Arumugam, A. R. Inigo, A. L. Kanibolotsky, R. W. Martin and P. J. Skabara, *J. Mater. Chem. C*, 2013, **1**, 2249–2256.
41 S. Koltzenburg, M. Maskos and O. Nuyken, *Polymer Chemistry*, Springer-Verlag, Berlin Heidelberg, 2017.